

1 **A COMPARATIVE STUDY OF GEOPOLYMERS SYNTHESIZED FROM OXY-**
2 **COMBUSTION AND CHEMICAL LOOPING COMBUSTION BOTTOM ASHES**
3

4 C.N Nkuna¹, *B.O Oboirien^{1,2}, E.R Sadiku¹ and J Lekitima³

5 ¹*Tshwane University of Technology Department of Chemical, Metallurgical and Materials*
6 *Engineering Pretoria, South Africa*

7 ²*CSIR Material Science and Manufacturing, Pretoria, South Africa*

8 ³*Department of Chemistry, University of Pretoria South Africa*

9 **Abstract**

10 The generation of geopolymers from OXY-FBC and CLC bottom ashes has not yet been
11 reported. In this study, geopolymers from OXY-FBC and CLC bottom ash were synthesised
12 and compared with geopolymers from FBC bottom ash. The bottom ashes used in this study
13 were generated from the combustion of high ash South African coal. FBC and OXY-FBC
14 bottom ashes were divided into two, viz: the first half was coarse, while the second half was
15 grinded into fine particles. The bottom ashes were mixed with sodium silicate (Na₂SiO₂) and
16 sodium hydroxide solutions (5M, 10M and 15M) and the pastes were cured at 60°C for 10
17 days. The properties of the geopolymers were characterized using: TGA, FTIR and SEM-
18 EDX techniques. TGA analysis showed that FBC geopolymer with 5M NaOH had the least
19 amount of % weight loss, which indicates that it had a better thermal stability than
20 synthesizing geopolymers with higher NaOH concentrations. Coarse FBC geopolymer (C-
21 A1) had a higher thermal stability than fine FBC geopolymer (F-B1), therefore indicating that
22 there is no need to grind the ash. OXY-FBC showed the opposite, therefore indicating the
23 need to grind the ash in order to attain a better thermal stability of the geopolymer. The EDS
24 analysis showed that the geopolymers produced an N-A-S-H gel and an incomplete N-A-S-H
25 gel, instead of the C-(A)-S-H gel. Geopolymers synthesized from 5M NaOH (C-A1, F-B1
26 and C-C1), 10M NaOH (F-D2) and 15M NaOH (F-E3) had the most degree of
27 geopolymerisation as seen on the FTIR spectrum. Geopolymers (F-D2) synthesized from
28 10M NaOH and fine OXY-FBC bottom ash had greater degree of geopolymerisation.

29
30 **Keywords:** Oxy-FBC, chemical looping combustion, bottom ash, geopolymers
31
32
33
34
35
36
37

1. Introduction

The depletion of high quality coals has resulted in the growth of the combustion of low grade coals for power. Fluidized bed combustors (FBC) are better suited for low grade coals because of its low operating temperature (800-950°C) [1]. However, there is still the production of greenhouse gases, such as carbon dioxide (CO₂). The CO₂ emission can be reduced by using fluidized bed combustor (Oxy-FBC), which recycles the CO₂ back into the boiler for better capture [2]. Oxy-FBC also produce lower NO_x and SO_x emissions when compared to Air-FBC process. The absence of nitrogen in the oxidant leads to a lower NO_x emissions[2]. Sulphur capture is higher in OXY-FBC than in Air-FBC because the high partial pressure of CO₂, in OXY-FBC prevents the calcination of limestone and there increasing the sorption capacity of the limestone. In Air-FBC the rate of calcination of the limestone is high and this reduces its sorption capacity [2].

Another CO₂ capture technology that is carried out under fluidised bed conditions, is Chemical looping combustion (CLC). CLC is a process where metal oxides are used to transport the oxygen between the two reactors, fuel reactor and air reactor [3-5]. In the fuel reactor the metal oxide reacts with the fuel to produce CO₂ and H₂O as fuel gases [(C_nH_n)_m + (2n+m)Me_xO_y → nCO₂ + mH₂O + (2n+m)Me_xO_{y-1}].The reduced metal oxide is transported into the air reactor in order to be oxidized by air [O₂ + 2Me_xO_{y-1} → 2Me_xO_y], then oxidized metal oxide is cycled back into the fuel reactor where it will be reduced to (cyclization process) oxides fuels while capturing CO₂. There is a lower energy penalty for CO₂ capture in CLC than in OXY-FBC .

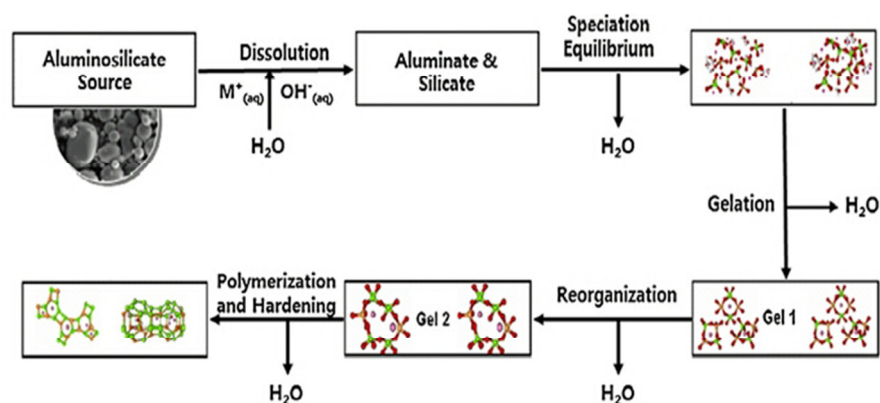
The bottom ashes generated from these CO₂ capture process (OXY-FBC and CLC) cannot be disposed to the environment (ground water and surface water) because of the enrichment of toxic trace elements in the ash samples. Font et al [6] reported that there was enrichment of Ca, Zr, Sb, Cr and V in coal ash generated from OXY-FBC process. Mendiara et al [7] reported that of Ni and Zn in coal ash generated from CLC process.

The production of geopolymers from the bottom ash can reduce or solve the waste disposal problem[8]. Coal bottom ashes have high content of silica and alumina are the key ingredients for the production of geopolymers[9].

69 Geopolymer is a synthetic inorganic alkali-activated aluminosilicates that is able to produce a
 70 Si-O-Al framework, which reacts and set rapidly at low temperatures resulting in a hard and
 71 stable product at high temperatures up to 1250°C [10] Geopolymers have a variety of
 72 applications, such as new ceramics and cements, matrices for hazardous waste stabilization,
 73 tooling and molding, fire-resistant materials and high-tech materials [11]. Geopolymerization
 74 reaction involved four steps and they involve the following [12]

- 75 i. dissolution of Al and Si oxides from the ash aluminosilicate due to the strong alkaline
- 76 liquid attack caused by sodium hydroxide and sodium silicate,
- 77 ii. formation of oligomer bonds such as Si-O-Si and Si-O-Al by polymerization
- 78 iii. formation of three dimensional aluminosilicate structures by the polycondensation of
- 79 the oligomers and
- 80 iv. bonding of the remaining unreactive solid filler particles to the aluminosilicate
- 81 network, to further enhance its strength and thermal stability

82 The reaction mechanism is illustrated in Figure 1 below[13].



83
84

Figure 1: The reaction mechanism of geopolymerisation.[10-11]

85 The generation of geopolymers from Oxy-FBC and CLC bottom ashes has not been reported.
 86 The main objective of this study is to compare the properties of the geopolymer precursors
 87 produced from OXY-FBC, CLC and FBC bottom ashes. The degree of geopolymerisation
 88 was determined by FTIR, TGA and SEM-EDS analyses.

89

90

91

92 2. Experimental

93 2.1 Materials

94 The bottom ash was generated from the combustion of a high ash South African coal from
95 FBC, OXY-FBC and CLC processes using a bubbling fluidised bed reactor. Full details of
96 this reactor and the experimental conditions for bottom ash generation can be found in
97 Mathekga et al. [12] FBC and OXY-FBC bottom ashes were divided into two halves, one
98 half was grinded into fine particles (75 microns) and the other half was kept as coarse
99 particles (600 microns). CLC bottom ash was grinded into fine particles (75 microns). An
100 analytical grade of sodium hydroxide was prepared by mixing the NaOH pellets with distilled
101 water in order to make 5M, 10M and 15M NaOH solutions, which were used as alkali fusion
102 pre-treatment for the bottom ash. An industrial grade 3379 of sodium silicate (29.80% SiO₂,
103 9.16% Na₂O and 61.04% H₂O) was used for the preparation of the activating solution
104 together with the prepared NaOH solutions [13-14]. The specific gravity of sodium silicate
105 was 1.39g/cm³.

106 2.2 Sample preparation

107 Fifteen geopolymer precursors (6 FBC, 6 OXY-FBC and 3 CLC) were prepared from mixing
108 the activating solution (NaOH:Na₂SiO₃) with the ash for 7 minutes until a homogeneous
109 mixture was obtained.^[13] The activating solution was kept at a ratio of 1. Tables 1 and 2
110 indicate the proportions (ratios) in which the activating solution was mixed with the ash in
111 order to obtain the geopolymer precursors. The C-A's and C-C's are coarse bottom ash from
112 FBC bottom ash and OXY-FBC bottom ash, respectively, while the F-B's, F-D's and F-E's
113 are the fine bottom ash from FBC bottom ash, OXY-FBC bottom ash and CLC bottom ash,
114 respectively. The geopolymer precursors produced were poured into cubic polypropylene
115 trays and the trapped air bubbles were removed by vibrating the polyethylene tray. The mold
116 trays were then sealed with polyethylene film (to prevent moisture loss) and set in the oven at
117 60°C for 48 hours, which was the initial curing [15]. After the initial curing, the sample were
118 demoulded and then returned into the oven for the second curing for 192 hours at 60°C,
119 making a total curing time in the oven at 60°C of 10 days.[15] The geopolymer precursors
120 were then cured at room temperature for 10 days after the 10 days curing in the oven was
121 completed.

122

123

124

125 Table 1: The mixing ratios for the geopolymer precursors synthesized from coarse bottom

126

ashes

Precursors	C-C1	C-A2	C-A3	C-C1	C-C2	C-C3
[NaOH]	5M	10M	15M	5M	10M	15M
Bottom ash	FBC	FBC	FBC	OXY	OXY	OXY
Ash:Activation solution	1	1	1	1	1	1

127

128 Table 2: The mixing ratios for the geopolymer precursors synthesized from fine bottom

129

ashes

Precursors	F-B1	F-B2	F-B3	F-D1	F-D2	F-D3	F-E1	F-E2	F-E3
[NaOH]	5M	10M	15M	5M	10M	15M	5M	10M	15M
Bottom ash	FBC	FBC	FBC	OXY	OXY	OXY	CLC	CLC	CLC
Ash: Activation solution	1	1	1	1	1	1	1	1	1

130

131

2.3 Analysis

132 Geopolymer precursors were analyzed with: FTIR, TGA and SEM coupled with EDS.

133 Fourier transformation infrared spectroscopy (FTIR) was performed with a Perkin Elmer

134 spectrum RX FT-IR system, the samples were analyzed using the KBr pellet technique (3mg

135 powder sample mixed with 100mg of KBr) [16]. Thermo-gravimetric analysis (TGA) was

136 conducted with Perkin Elmer TGA 7, with ~10mg per sample analyzed between the

137 temperature range of 30-1000°C in a nitrogen gas atmosphere, at a heating rate of 20°C per

138 minute [16-17] Scanning electron microscopy (SEM), coupled with energy dispersive X-ray

139 spectrometer (EDS) was used for the study of the sample morphology, with the sample

140 coated with gold particles in order to improve conductivity [16-18].

141

142

143 3. Results

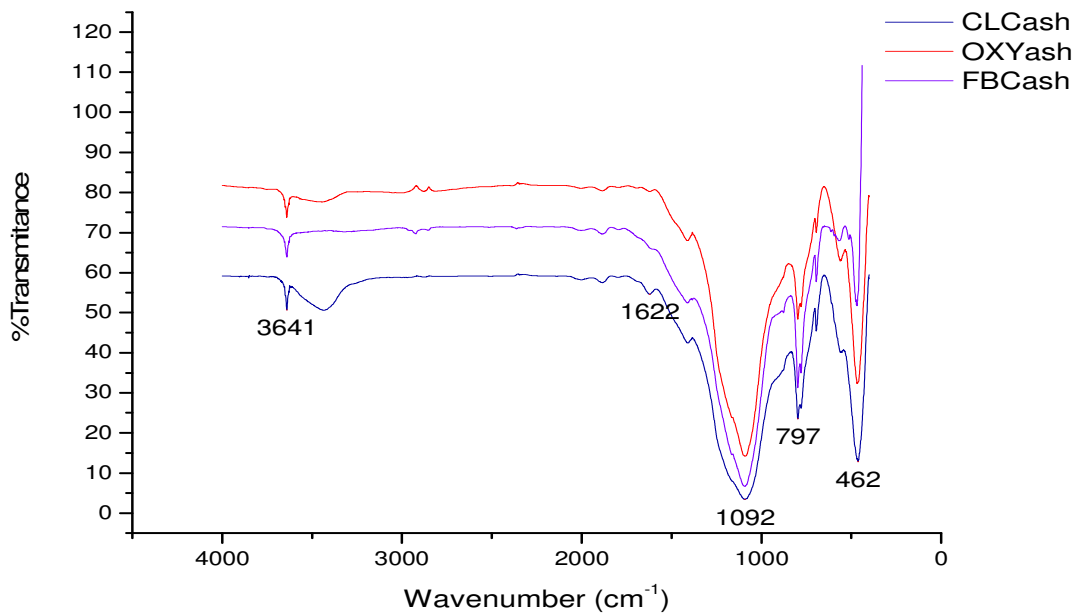
144 3.1. FTIR spectrums for the raw bottom ashes and the synthesised geopolymers

145 Table 3 indicates the type of vibrational modes which are present on the spectra of observed
146 of the geopolymers and the range at which each mode vibrates (wavenumbers). The FTIR
147 spectrum shows the effectiveness of geopolymerisation by revealing the peaks that are not
148 present in the bottom ash, but are very prominent in the geopolymer. Figure 2 shows the
149 comparison between the bottom ashes spectra and it can be seen from the figure that there is
150 not a lot of difference in the spectra when they are superimposed on each other. FBC bottom
151 shows a broad peak of Si-O-Si at 1091cm^{-1} , while CLC shows a more prominent peak at
152 461cm^{-1} of the Si-O-Si group than the other ashes (seen in Table 3), following rearrangement
153 to form Si-O-Al during geopolymerisation. All the three ashes have no prominent peaks of
154 CO_2 and H_2O , which signifies the formation of geopolymers.

155 Table 3: The chemical composition of the geopolymer precursor and the bottom ash obtained
156 from a FTIR spectrum

Wavenumber (cm^{-1})	Modes
450-460	Si-O-Si and O-Si-O vibrational bending
675-685	Si-O-Si and Al-O-Si symmetric stretching
770-780	Si-O-Si symmetric stretching
880	Si-O stretching
980-1100	T-O-Si (T=Si or Al) Asymmetric stretching
1400-1460	CO_2 vibrational stretching (atmospheric carbonation)
1500-1600	H-O-H vibrational bending
2300-3500	(-OH) vibrational stretching

157



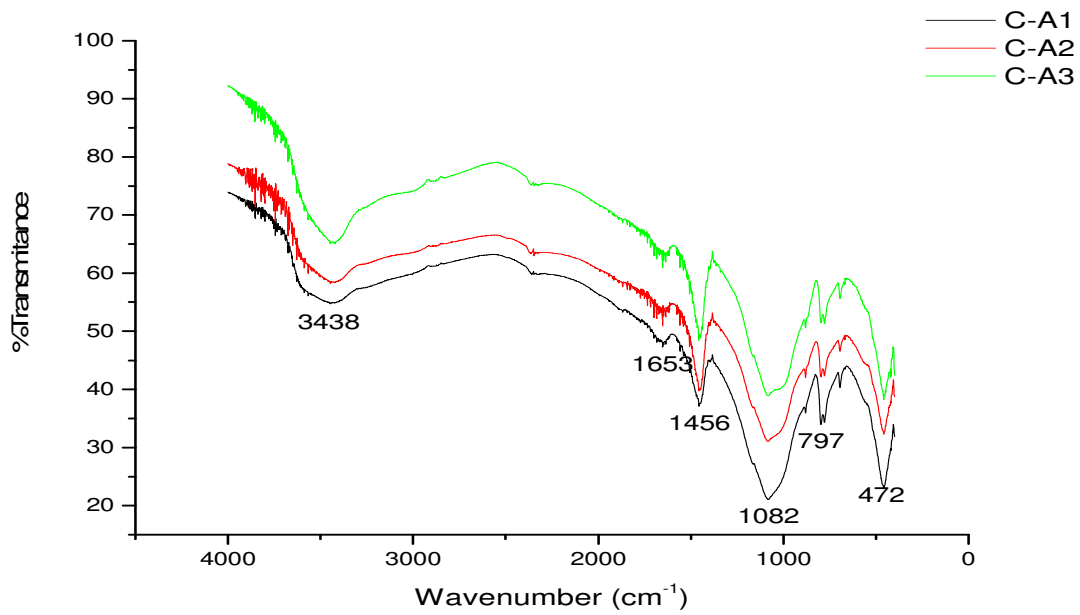
158

159

Figure 2: The infrared spectrum for the bottom ashes

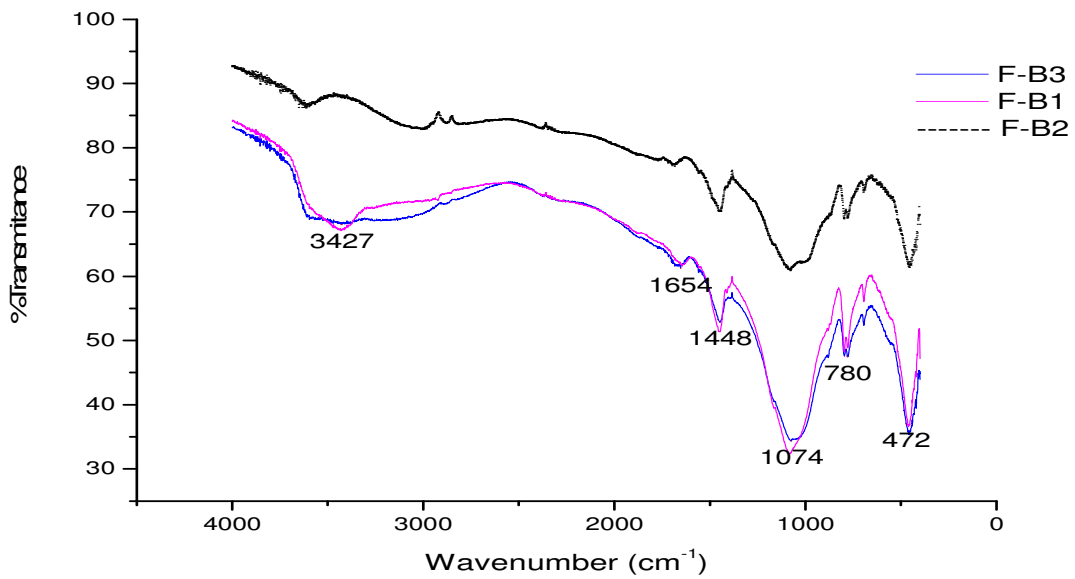
160 The infrared spectra for geopolymers synthesised from the coarse FBC bottom ash, using
 161 different NaOH concentrations are presented in Figure 3. The result shows that there is
 162 evidence of geopolymerisation as seen from the presence of prominent peaks at 1460cm^{-1} for
 163 $\text{O}=\text{C}=\text{O}$, 1645cm^{-1} which indicates the presence of water absorbed (H-O-H bending
 164 vibration) and the broad band of T-O-Si (T=Si or Al) asymmetric stretching as a
 165 consequence of polycondensation with alternating Si-O or Al-O (T=Si or Al), which are not
 166 prominent in the Figure 2 for the FBC bottom ash C-A1 with 5M NaOH had the most
 167 prominent/broad peaks at the indicated wavenumbers, which signifies geopolymerisation and
 168 indicating the fact that more geopolymerisation took place with 5M NaOH than the other
 169 NaOH concentrations.

170 The infrared spectra of the geopolymers synthesised from fine FBC bottom ash using
 171 different NaOH concentrations are presented in Figure 4. F-B1 with 5M NaOH has the most
 172 prominent/sharp peak at 1074cm^{-1} , and the highest degree of geopolymerisation. **Similar**
 173 **result was reported in the literature for a blend of fly ash and bottom ash from a circulating**
 174 **fluidised bed reactor [15]. They obtained an increase in the broadness of bands 1095 cm^{-1} and**
 175 **1089 cm^{-1} in the FTIR spectra using a 5M NaOH solution.**



176

177 *Figure 3: Infrared spectrum for geopolymers synthesized from coarse FBC bottom ash*

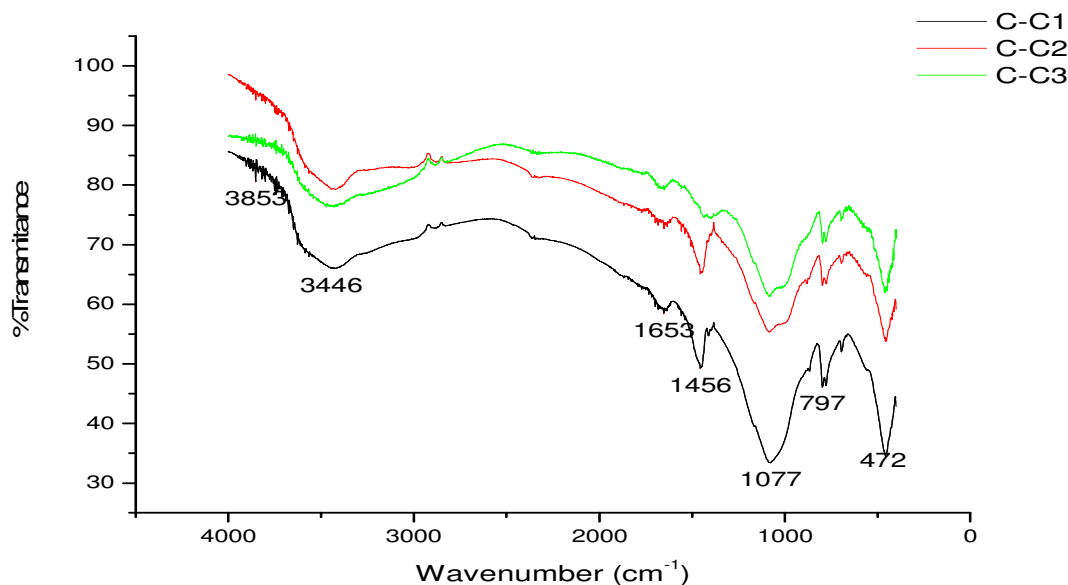


178

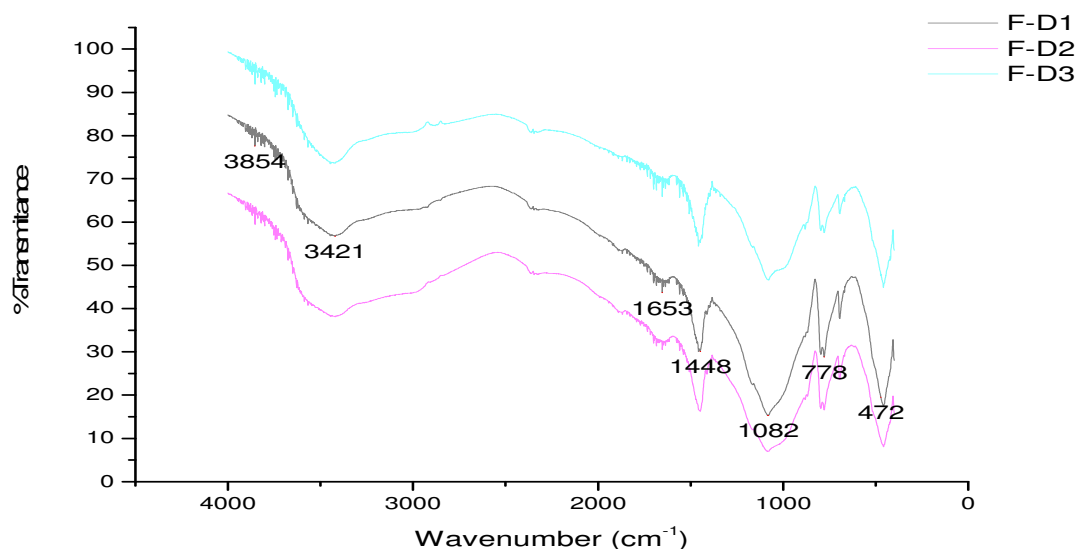
179 *Figure 4: Infrared spectrum for geopolymer synthesized from coarse FBC bottom ash*

180 The FTIR spectra of the geopolymers synthesized from coarse and fine OXY-FBC bottom
 181 ashes are shown in Figures 5 and 6, respectively. It can be clearly seen that there is a degree
 182 of geopolymerisation, since there are prominent peaks of CO₂ vibrational stretching, H-O-H
 183 vibrational bending and -OH vibrational stretching, which are not prominent in the OXY-

184 FBC ash[7-8]. The geopolymers synthesized from coarse bottom ash C-C1 with 5M NaOH
 185 had the most prominent/sharp peak at 1077cm^{-1} , therefore indicating a higher degree of
 186 geopolymerisation than in C-C2 and C-C3 ashes. The geopolymers synthesized from fine
 187 bottom ash F-D2 with 10 M NaOH had the most prominent peak at wavenumber 1082cm^{-1}
 188 than the other geopolymer precursors (F-D1 and F-D3), therefore indicating that F-D2 had
 189 the most 3D network structure being formed.

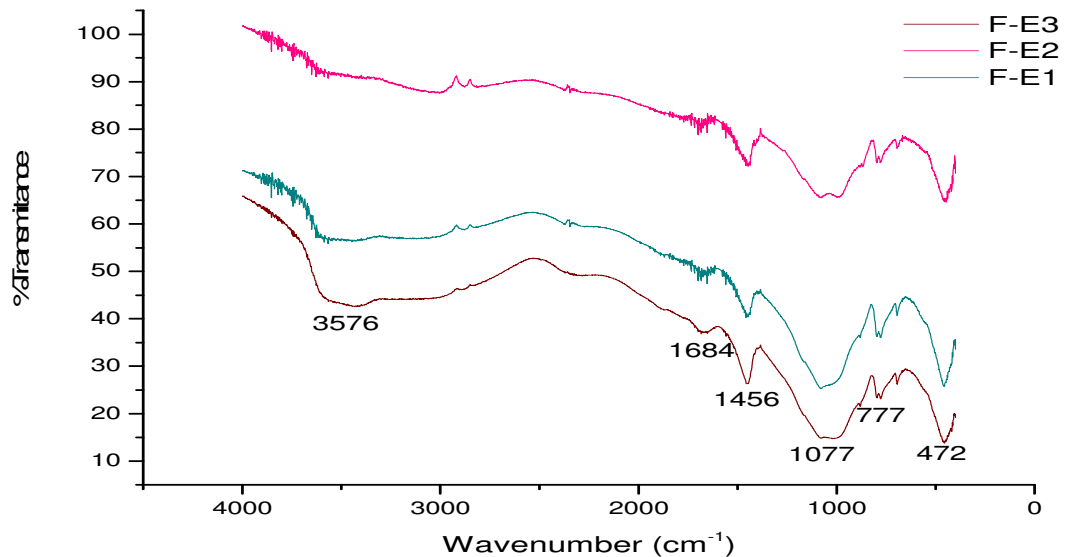


190
 191 *Figure 5: Infrared spectrum for geopolymers synthesized from coarse OXY-FBC bottom ash*



192
 193 *Figure 6: Infrared spectrum for geopolymers synthesized from fine OXY-FBC bottom ash*

194 The spectra in Figure 7 show that the peaks for CO₂ and H-O-H were more prominent for the
195 geopolymer than for the CLC bottom ash shown in Figure 2. Between the three geopolymers,
196 F-E3 had the most prominent peaks, indicating the fact that geopolymers synthesized from
197 15M NaOH resulted in greater degree of geopolymerisation than those synthesized with low
198 NaOH concentration.



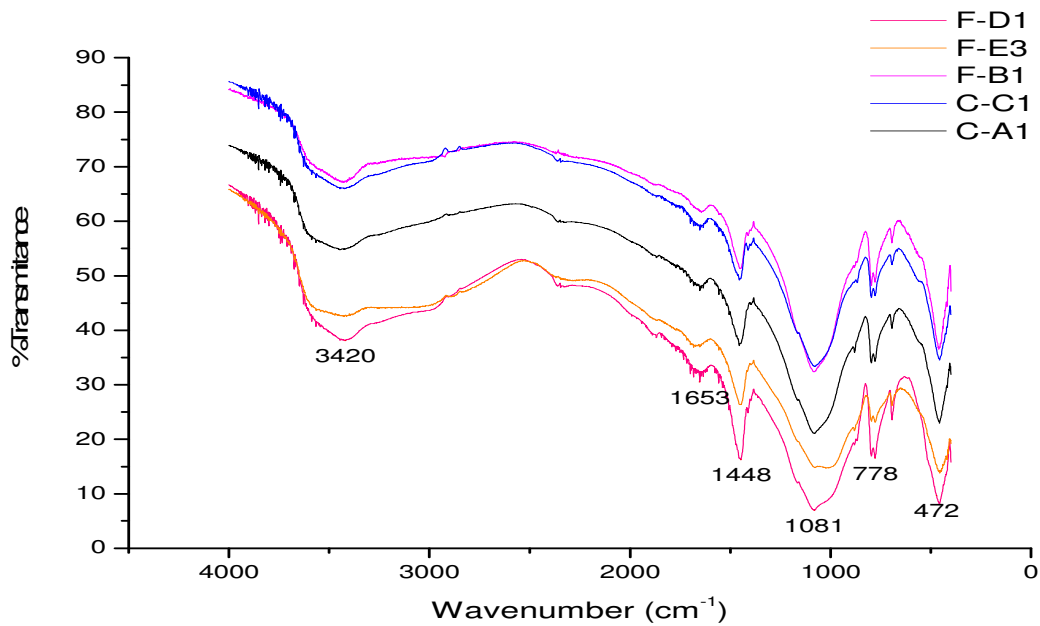
199

200 *Figure 7: The infrared spectrum for geopolymers synthesized from CLC bottom ash*

201

202 A comparison of the best conditions for the various geopolymers synthesized from coarse
203 and fine bottom ashes of FBC, OXY-FBC and fine bottom ash from CLC is presented in
204 Figure 8. From the spectra, it can be seen that F-D2 had the most prominent peaks at 1081cm⁻¹
205 and 1446cm⁻¹, which indicate a good degree of geopolymerisation and therefore confirming
206 the fact that fine OXY-FBC bottom ash with 10M NaOH produced the best geopolymer than
207 the other geopolymer precursors.

208



209

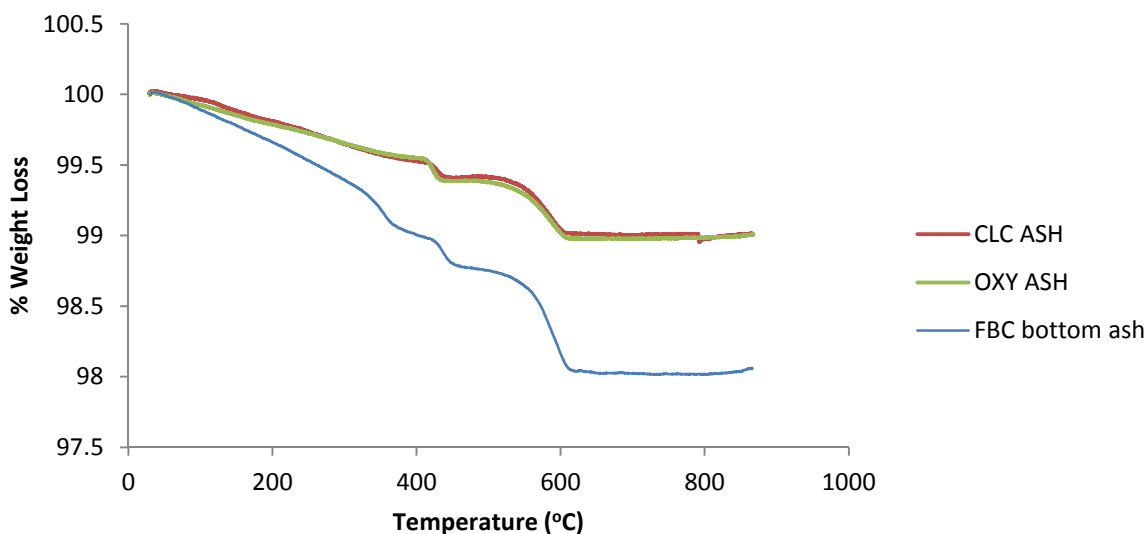
210 *Figure 8: Comparison of infrared spectrum for geopolymers with the most degree of*
 211 *polymerisation*

212

213 3.2 The TGA analysis for geopolymers synthesized from bottom ashes

214 **The thermal stability of the geopolymers were evaluated by a TGA.** The reduction in weight
 215 loss was due to the loss of water during the curing of the geopolymer precursors at 60°C. At
 216 temperature below 250°C, a certain degree of weight loss is attained, while the remaining
 217 water was either tightly bounded or less able diffuse to the surface of the geopolymer,
 218 therefore continues to evolve at higher temperature, above 250°C in a dehydration reaction,
 219 where it is lost as gas $[2(\text{SiO}_3^{2-} \cdot 2\text{M}^+) \rightarrow (\text{SiO}_3^{2-} \cdot 2\text{M}^+)_2 + \uparrow\text{H}_2\text{O}(\text{g})]$ [16, 20-21]. The three
 220 bottom ashes had a similar % weight loss trend, except for the FBC bottom ash that has a 2%
 221 weight loss, while CLC and OXY-FBC bottom ashes had 1% and 1.1%, respectively, as seen
 222 in Figure 9.

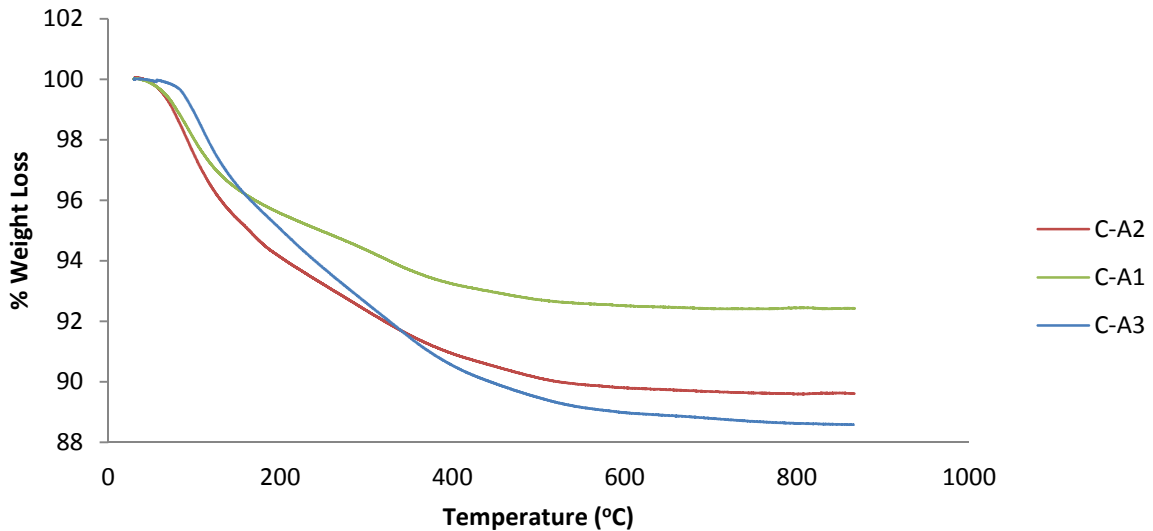
223



224

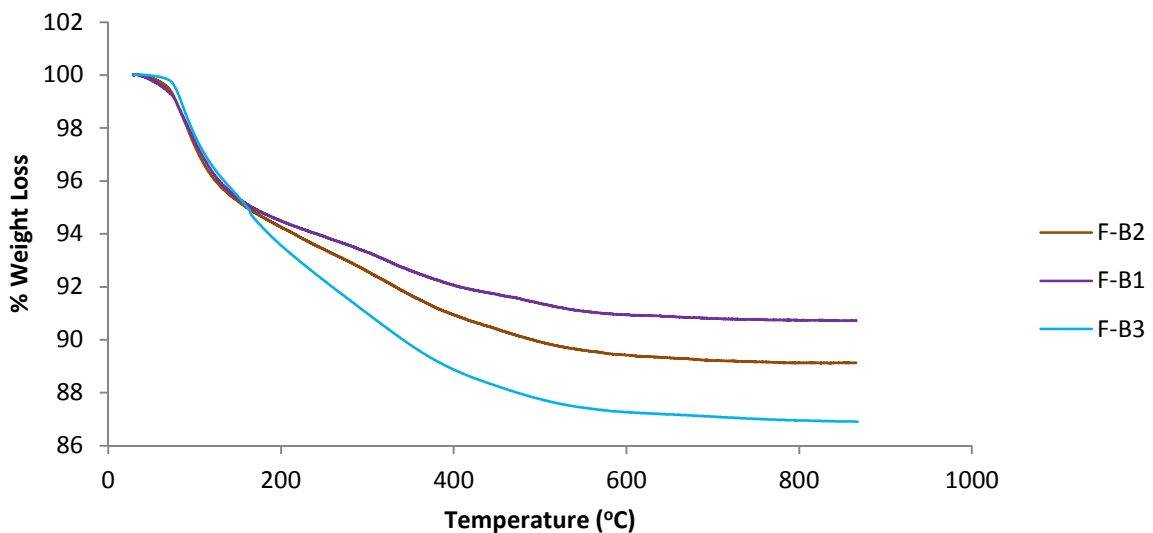
225 *Figure 9: Comparison of the % weight loss of the three bottom ashes*

226 Figures 10 and 11 show the weight losses for the coarse and fine geopolymer precursors,
227 respectively. The results were similar. The coarse FBC geopolymers, C-A1 (5M NaOH) had
228 the least amount of weight loss of 5% at <250°C and a 3% weight loss, as gas at higher
229 (>250°C) temperature. C-A2 (10M NaOH) and C-A3 (15M NaOH) had lost ~11% and
230 11.6%, respectively with 6% loss at <250°C, while the rest of the water lost as gas at higher
231 (>250°C) temperature. The fine FBC geopolymers, F-B1 (5M NaOH) had the least amount of
232 weight loss with a total of 9.2%. F-B2 and F-B3 had 11.8% and 14.2% weight losses,
233 respectively, where 6.5% of water was lost <250°C, while the rest of the water evolved as gas
234 at higher (>250°C) temperature. As a group, geopolymers synthesized from coarse FBC
235 bottom ash had a lower weight loss when compared with geopolymers synthesized from fine
236 FBC bottom ash and therefore, indicating the fact that coarse FBC geopolymers had a better
237 thermal stability and hence, it is unnecessary to grind the FBC bottom ash before its synthesis
238 into geopolymers.



239

240 *Figure 10: Comparison of % weight loss of geopolymers precursors synthesized from coarse*
 241 *FBC bottom ash*

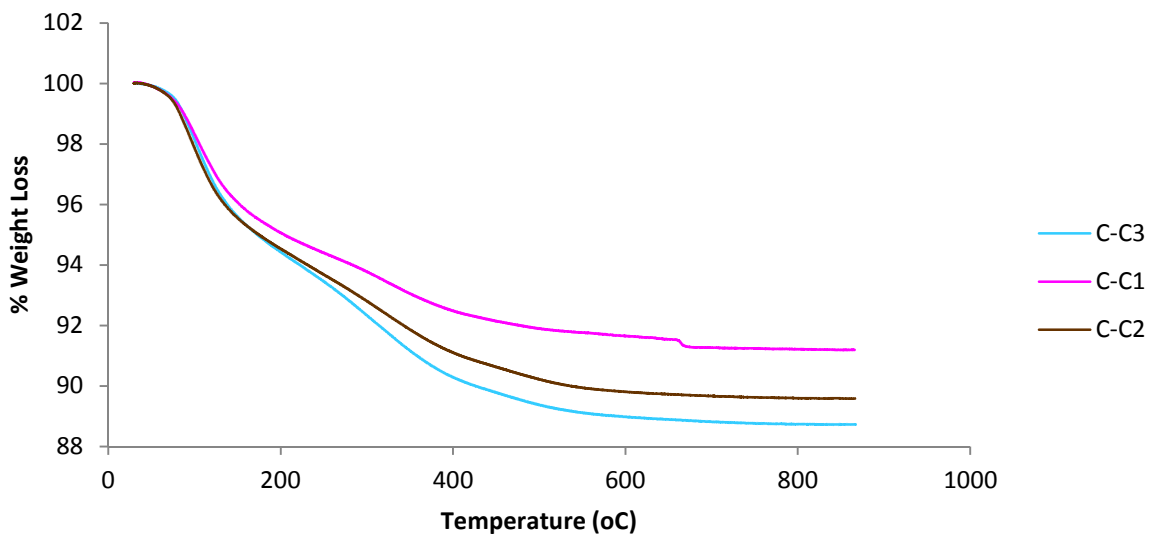


242

243 *Figure 11: Comparison of % weight loss of geopolymers precursors synthesized from fine*
 244 *FBC bottom ash*

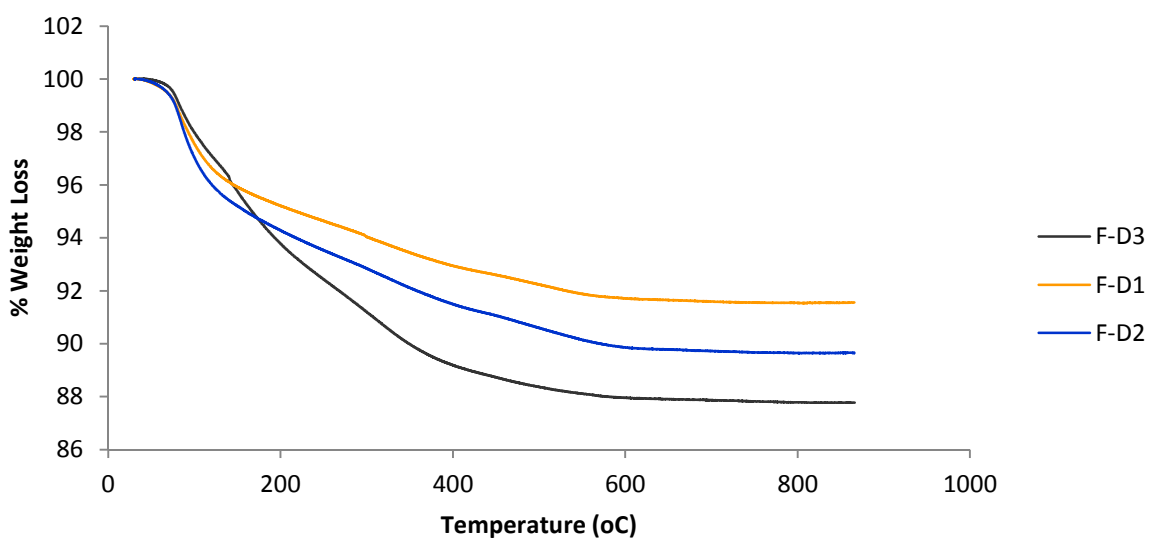
245 The % weight loss for geopolymers synthesized from the coarse and fine OXY-FBC ashes
 246 (Figure 12 and 13) had similar thermal stability as the FBC geopolymers (Figures 9 and 10).
 247 Geopolymers synthesized with 5M NaOH from the coarse (C-C1) and fine (F-D1) OXY-FBC
 248 ashes, had the least amount of weight loss during curing at 60°C, as seen in Figures 12 and
 249 13. F-D1 had the least amount of weight loss when compared with C-C1 (8.4% and 8.8%,
 250 respectively), therefore F-D1 exhibited a better thermal stability than C-C1, which shows that

251 there is a need to grind the OXY-FBC bottom ash before geopolymers synthesis.
252 Geopolymers synthesized with 10M NaOH from the coarse(C-C2) and fine (F-D2) OXY-
253 FBC bottom ashes, had the same amount of weight loss of ~10.4%, indicating the fact that
254 their thermal stability is the same. Geopolymers synthesized with 15M NaOH from the coarse
255 (C-C3) and fine (F-D3) OXY-FBC bottom ashes, showed that fine OXY-FBC geopolymer
256 (C-C3) had better thermal stability than F-D3, since the weight losses were 11% and 12.4%,
257 respectively.



258

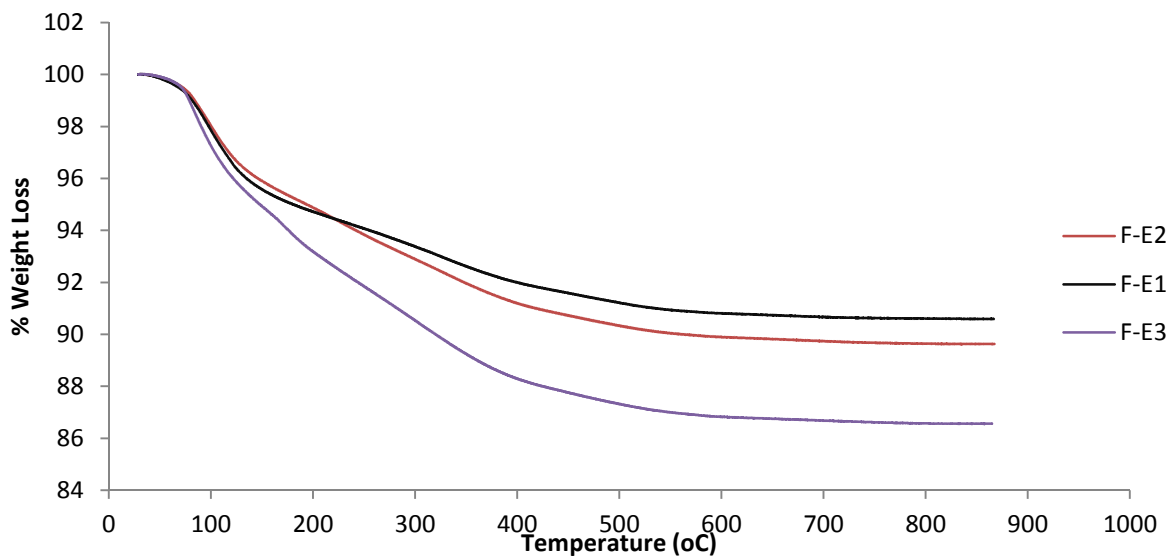
259 *Figure 12: Comparison of % weight loss of geopolymer precursors synthesized from coarse*
260 *OXY-FBC bottom ash*



261

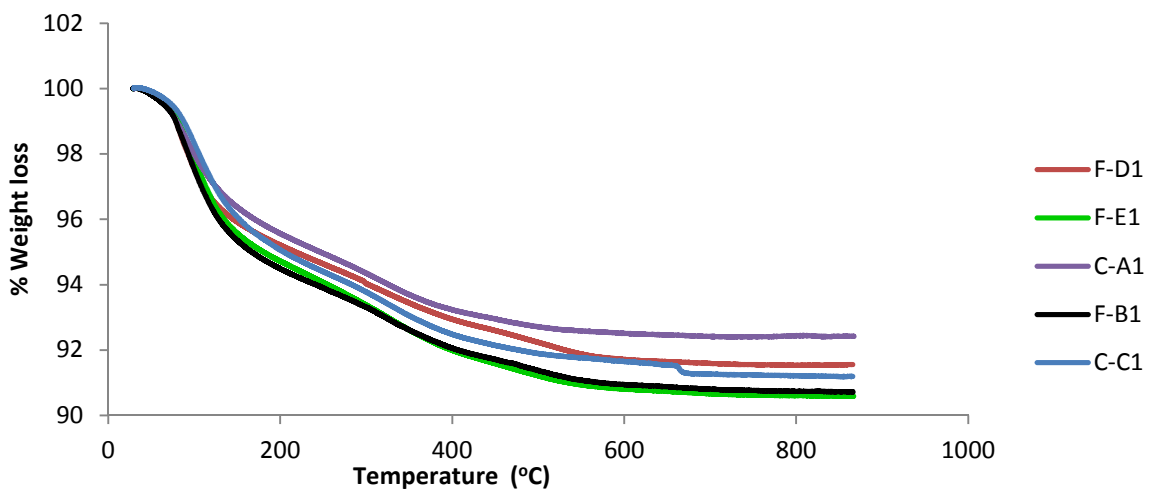
262 *Figure 13: Comparison of % weight loss of geopolymer precursors synthesized from fine*
263 *OXY-FBC bottom ash*

264 Figure 14 shows the weight losses of fine CLC geopolymer precursors and F-E1 (5M NaOH)
265 had the a least amount of weight loss than CLC geopolymer precursors synthesized at higher
266 temperatures. F-E1 had about 9.2% weight loss which is the same as F-B1 weight loss, while
267 F-E2 had about 10.8% and F-E3 had about 13.2%. F-E1 had a better thermal stability,
268 indicating the fact that CLC bottom ash requires low NaOH concentration in order to produce
269 geopolymer with good thermal stability.



270

271 *Figure 14: comparison of % weight loss of geopolymer precursors synthesized CLC bottom*
272 *ash*



273

274 *Figure 15: comparison of geopolymer precursors with the least % weight loss*

275 Figure 15 shows the comparison between the geopolymer precursors with the least weight
 276 loss, which will help in the identification of the geopolymer with the highest thermal stability.
 277 Geopolymers synthesized with 5M NaOH had greatest thermal stability than those
 278 synthesized with higher NaOH concentrations. F-E1 and F-B1 had the same weight loss,
 279 hence they are superimposed on each other, as seen in Figure 15. C-A1 had the least weight
 280 loss, indicating a better thermal stability than the rest of the geopolymers and therefore, it can
 281 be inferred that coarse FBC bottom ash produces a better geopolymer.

282 3.3 SEM and EDS results for geopolymers synthesized from bottom ash

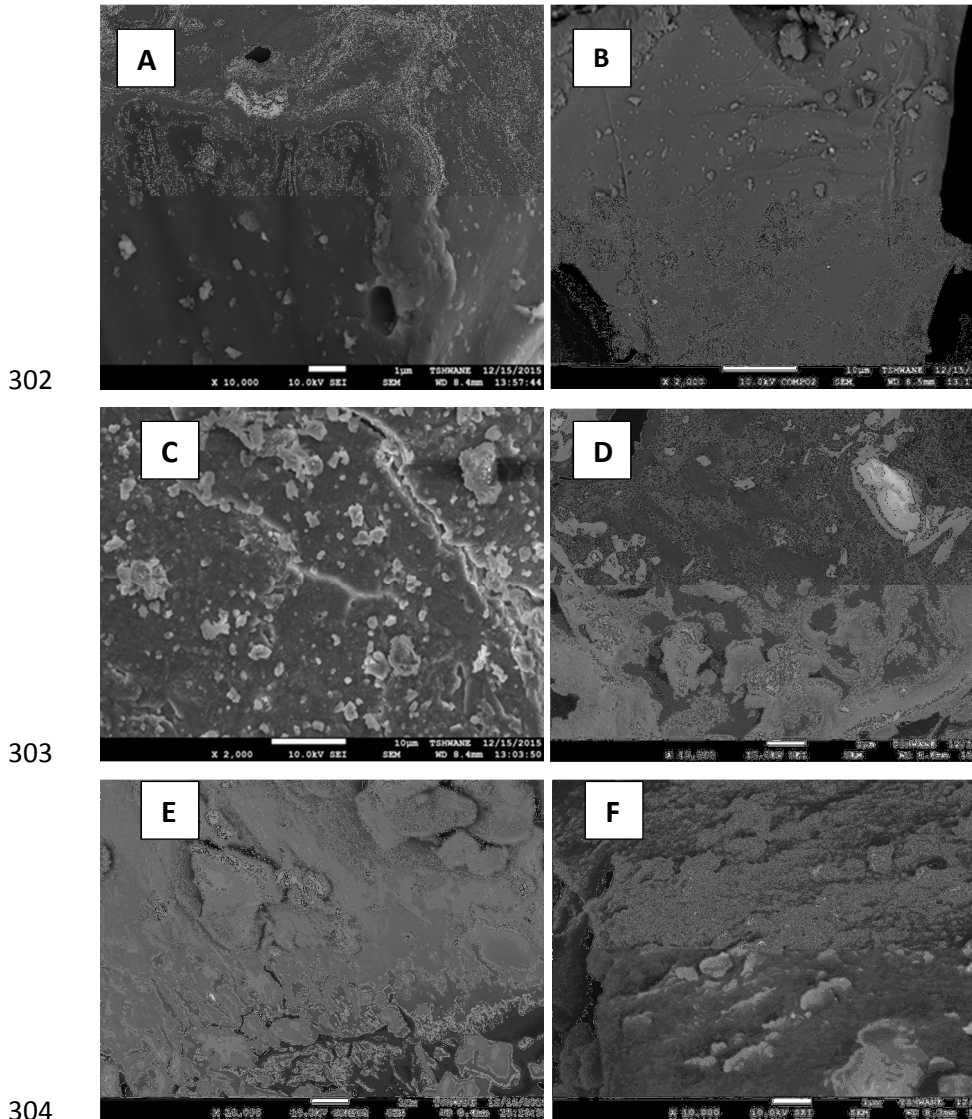
283 SEM-EDS analysis is one of the tools used in evaluating the microstructural properties of
 284 geopolymers. The morphology of geopolymers is evaluated using the SEM analysis and the
 285 elemental composition of the geopolymer is evaluated by doing the EDS analysis. The EDS
 286 analysis for geopolymers synthesized from air-FBC bottom ash is presented in Table 3 and
 287 based on the composition of the geopolymer, it has an N-A-S-H gel[22-23] The Si/Na ratio of
 288 geopolymers (C-C1-3) synthesized from coarse FBC bottom ash is greater than 2, therefore,
 289 indicating a moderate degree of reaction in the system due to the high content of unreacted
 290 Si[22-23]. C-A1 had a higher Si/Al ratio, indicating that it should result in a high
 291 compressive strength[22-23]. Fine FBC geopolymer precursors resulted in an incomplete N-
 292 A-S-H gel since the Si/Na ratio was greater than 1, therefore there was a moderate degree of
 293 geopolymerisation reaction.

294 Table 3: EDS data for geopolymers synthesized from FBC bottom ash

	O	Na	Al	Si	P	K	Ca	Mg	Si/Al	Si/Na	Na/Si
C-A1	53.75	5.65	5.75	23.71	1.78	0.26	0.37	-	4.12	4.19	0.24
C-A2	60.21	3.07	8.67	23.48	1.29	0.28	-	-	2.71	7.65	0.13
C-A3	49.62	7.74	15.37	21.03	0.96	0.84	-	0.28	1.37	2.72	0.37
F-B1	59.08	5.21	1.99	28.45	0.77	0.29	2.15	-	14.30	5.46	0.18
F-B2	45.85	9.28	11.80	14.13	0.91	1.42	2.84	-	1.20	1.50	0.66
F-B3	45.75	10.25	5.86	29.31	0.50	-	2.48	-	5	2.86	0.35

295

296 Based on Figure 16, it is clearly seen that an incomplete N-A-S-H gel was formed for
297 geopolymers synthesized from coarse FBC bottom ash, since there are unreacted particles on
298 the geopolymer surface [24-25]. C-C3 had cracks on the surface due to the extra water
299 retained during curing [24-25]. From Figure 16-f, it can be seen that the surface of F-B3
300 geopolymer is similar to the incomplete N-A-S-H gel in F-B1 and F-B2 with large unreacted
301 Si or Al particles.



305 *Figure 16: SEM morphology of FBC coarse and fine geopolymer precursors; (a) C-A1 with*
306 *5M NaOH, (b) C-A2 with 10M NaOH, (c) C-A3 with 15M NaOH, (d) F-B1 with 5M NaOH,*
307 *(e) F-B2 with 10M NaOH and (f) F-B3 with 15MNaOH*

308

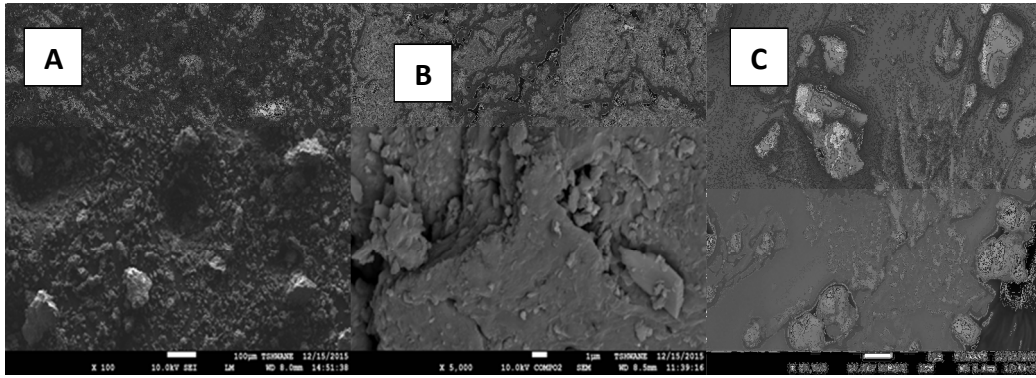
309

310 Table 4: EDS data for geopolymers synthesized from OXY-FBC bottom ash

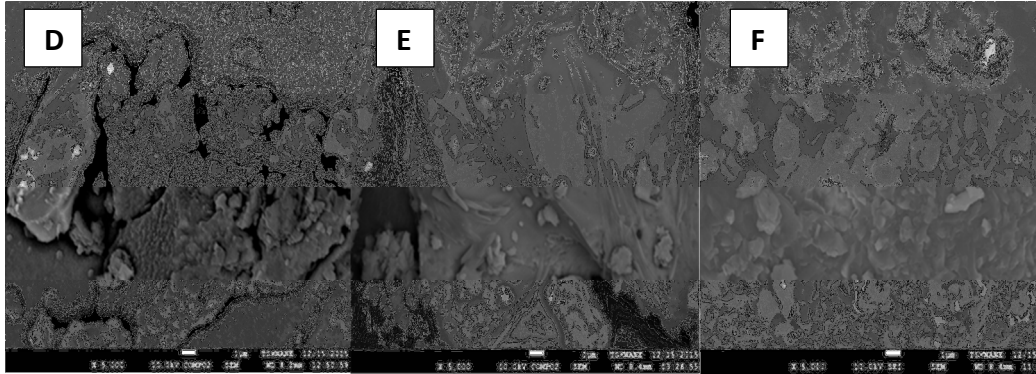
	O	Na	Al	Si	P	K	Ca	Br	Si/Al	Si/Na	Na/Si
C-C1	51	4.75	11	15.99	-	-	-	-	1.45	3.37	0.30
C-C2	50.88	12.86	3.24	24.24	-	0.27	0.40	-	7.08	1.88	0.53
C-C3	52.55	13.30	10.36	11.48	-	0.31	-	-	1.11	0.89	1.12
F-D1	28.43	3.45	51.81	-	2.75	-	-	3.93	-	-	-
F-D2	43.04	7.36	1.13	34.79	0.96	-	-	-	30.79	4.73	0.21
F-D3	53.83	18.38	1.36	16.33	0.96	-	3.72	-	12	0.89	1.13

311

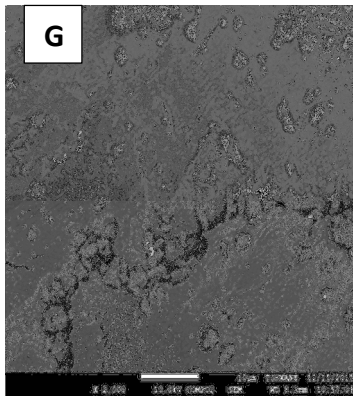
312 Table 4 shows that geopolymers synthesized from OXY-FBC bottom ash had three
 313 incomplete N-A-S-H gels formed, viz: C-S-H gel and two compact amorphous N-A-S-H
 314 structures. C-C1, C-C2 and F-D2 had an incomplete N-A-S-H gel formed since their Si/Na
 315 ratio was greater than 2, while C-C3 had Si/Na ratio which was approximately 1, therefore
 316 indicating a compact amorphous N-A-S-H structure had formed [22-23]. C-C2 is expected to
 317 have higher compressive strength since the Si/Al ratio is huge. F-D1 had resulted in a C-S-H
 318 gel structure, since there was zero content of Si, therefore forming aluminates structures. F-
 319 D2 had an incomplete N-A-S-H gel formed, while F-D3 had a compact amorphous N-A-S-H
 320 structure since the ratio of Si/Na was approximately 1 [22-24]. Oxy-FBC bottom ash had a
 321 diversity of ash particle sizes, with some being large while others were small as seen from
 322 Figure 17-a. Coarse OXY-FBC geopolymer (C-C1) had more cracks with particles of ash on
 323 the surface, which indicates an incomplete geopolymerisation [22-25]. C-C2 had few large
 324 ash particles on the surface. C-C3 had large particles of compared structure with few tiny ash
 325 particles on the surface. Fine OXY-FBC geopolymer prepared with 5M NaOH had crystal
 326 particles and large unreacted particles on the surface, which can be Al atoms, since zero
 327 content of Si was not detected by the EDS, as seen in Figure 17-e [22-23]. F-D2 had irregular
 328 surface, which indicates incomplete reaction of the geopolymerisation [22-25]. F-D3 had a
 329 large crack which resulted from the retention of more water during the curing of the
 330 material.^[22-26]



331



332



333

334 *Figure 17: SEM morphology of OXY-FBC ash and geopolymers; (a) Oxy-bottom ash, (b) F-*
 335 *D1 with 5M NaOH, (c) F-D2 with 10 M NaOH, (d) F-D3 with 15M NaOH, (e) C-C1 with 5M*
 336 *NaOH, (f) C-C2 with 10M NaOH and (g) C-C3 with 15M NaOH*

337

338

339

340

341

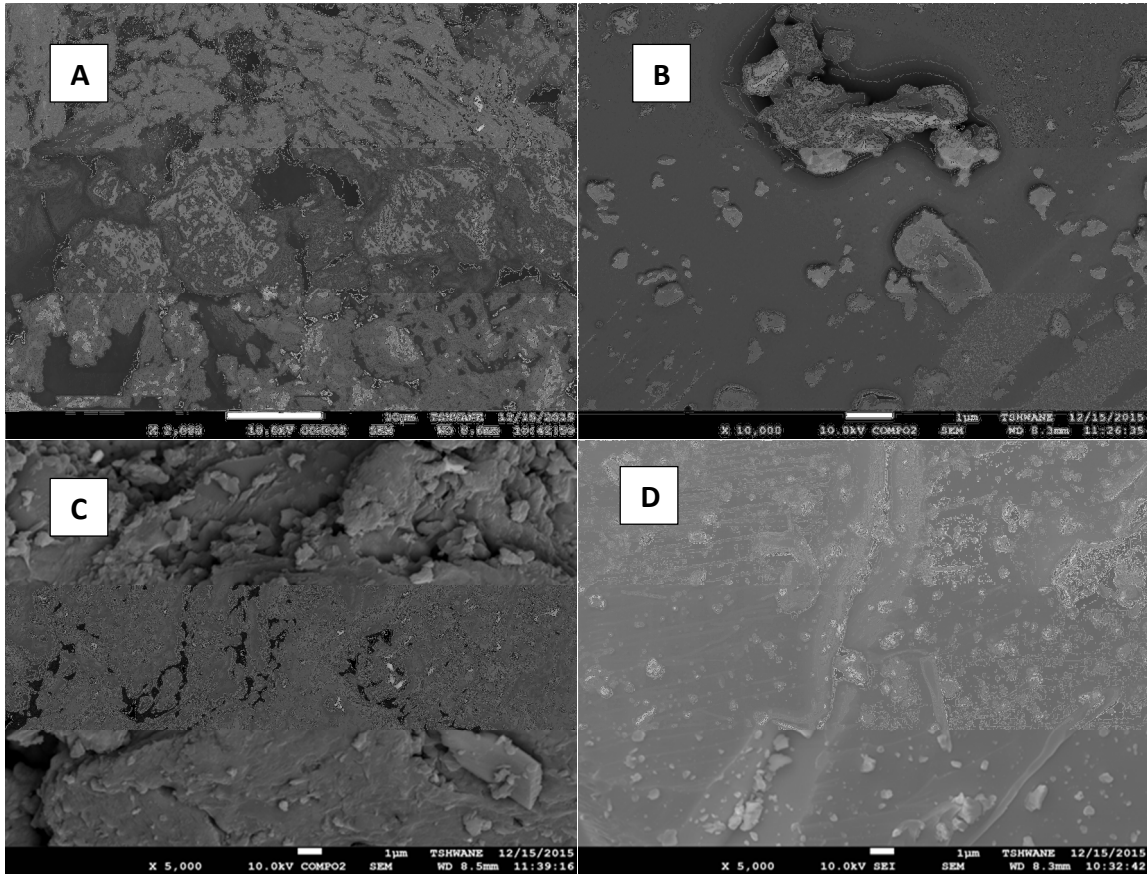
342

343 Table 5: EDS data for geopolymers synthesized from CLC bottom ash

	O	Na	Al	Si	K	P	Ca	Cu	Si/Al	Si/Na	Na/Si
F-E1	51.52	11.11	10.25	18.52	1.67	-	0.97	-	1.81	1.67	0.61
F-E2	50.79	2.54	4.98	33.25	1.53	-	-	2.39	6.68	13.09	0.08
F-E3	47.65	4.30	18.10	22.80	2.09	5.09	-	-	1.26	5.30	0.19

344

345 The CLC geopolymers had incomplete N-A-S-H gel being formed, since the Si/Na ratio for
 346 all three CLC geopolymers were greater than 1, as seen in Table 5. F-E2 had the most drastic
 347 incomplete N-A-S-H gel formed with Si/Na ratio of ~13.90, indicating the fact that the
 348 precursor paste solidified faster before the geopolymerisation could come to completion,
 349 which is seen by the high content of silica that forced the reaction not to come to completion
 350 [22-24]. F-E1 had a better N-A-S-H gel structure since its Si/Na ratio was not far from 1
 351 when compared with the other two CLC geopolymers [22-24]. F-E2 is expected to have a
 352 high compressive strength due to the high Si/Al ratio[22-24]. CLC bottom ash morphology
 353 showed large irregular particles with varied sizes and tiny pores on their surfaces, as seen in
 354 Figure 18-a [25-26]. F-E1 had many large cracks on the surface and many irregular particles,
 355 which are similar to the CLC ash in Figure 18-a. F-E2 had the most compact structure with
 356 large particles on the surface, while F-E3 had tiny particles (in size) on the surface with a
 357 large crack, as seen in Figure 18-c,d [25-26].



358

359

360 *Figure 17: SEM morphology of CLC ash and geopolymers; (a) CLC bottom ash, (b) F-E1*
 361 *with 5M NaOH, (c) F-E2 with 10M NaOH and (d) F-E3 with 15M NaOH*

362

363 **4. Application of geopolymer binders from FBC, OXY-FBC and CLC bottom**
 364 **ashes for the construction industry**

365 There might be a need for the blending of a more reactivity material such as metakaolin with
 366 FBC, OXY-FBC and CLC bottom ashes in the production of geopolymer for binders in the
 367 construction industry. This is due to an incomplete formation of a dense N-A-S-H gel, hence
 368 a low moderate degree of geopolymerisation. This was more prominent in the geopolymer
 369 synthesized from CLC bottom ash.

370

371

372 **Conclusions**

373

374 This study has proved that geopolymers can be synthesized from FBC, OXY-FBC and CLC
375 bottom ashes. Geopolymers synthesized from bottom ash has resulted in similar qualities as
376 geopolymers synthesized from fly ash. The use of different NaOH concentrations, has
377 resulted in a diversity of the degree of geopolymerisation. Geopolymers synthesized with 5M
378 NaOH (C-A1, F-B1 and C-C1), 10M NaOH (F-D2) and 15M NaOH (F-E3) had the most
379 degree of geopolymerisation, as seen in their FTIR spectra. Geopolymers (F-D2) synthesized
380 with 10M NaOH and fine OXY-FBC bottom ash had greater degree of geopolymerisation.
381 The EDS has shown that a N-A-S-H and an incomplete N-A-S-H gels had formed during the
382 geopolymerisation of the ashes at different NaOH concentrations. Only two geopolymers
383 synthesized from OXY-FBC bottom ash had resulted in amorphous compact N-A-S-H gels,
384 one synthesized from coarse OXY-FBC bottom at 15M NaOH and the other from fine OXY-
385 FBC bottom ash at 15M NaOH. The SEM images displayed a variety of complex structures
386 with most of them having particles on their surfaces and, some having large cracks which had
387 resulted in structural integrity being lost.

388 The thermal stability of the geopolymer precursors was analysed using TGA, where most of
389 the water was lost below 250°C, while the remaining water evolved as gas at
390 hightemperature. Geopolymers synthesized with 5M NaOH using FBC, OXY-FBC and CLC
391 bottom ashes (C-A1, F-B1, C-C1, F-D1 and F-E1) had the most thermal stability. C-A1
392 proved to have highest thermal stability, since it had lost the least amount of water, therefore
393 indicating the fact that FBC bottom ash does not need to be grinded before synthesis into
394 geopolymers. In the case of OXY-FBC geopolymers, the ash needs to be grinded since the
395 coarse OXY-FBC geopolymer (C-C1) retained more water than the fine OXY-FBC
396 geopolymer F-D1).

397

398

399

400

401

402 **5. References**

- 403 1. Basu P and Fraser SA. Circulating fluidized bed boilers: Design and operations.
404 USA. Butterworth-Heinemann. 1991. Pg 95-112 & 256-257
- 405 2. Wu Y, Wang C, Tan Y, Jai L and Anthony EJ.. Characterization of ashes from a
406 100kWth pilot scale circulating fluidized bed with oxy fuel combustion. Applied
407 Energy 2011. (88): 2940-2948
- 408 3. Lyngfelt A. Oxygen carriers for chemical looping combustion-4000h of
409 operational experience. Oil & Gas Science and Technology – Rev. IFP Energies
410 nouvelles 2011 (66): 161-172
- 411 4. Cormos CC, Cormos AM and Petrescu L. Assessment of chemical looping-based
412 conceptual designs for high efficient hydrogen and power co-generation applied to
413 gasification processes. Chemical Engineering Research and Design 2014. (92):
414 741-751
- 415 5. Hallberg P, Jing D and Rydén, M. Chemical Looping Combustion and Chemical
416 Looping with Oxygen Uncoupling Experiments in a Batch Reactor Using Spray-
417 Dried $\text{CaMn}_{1-x}\text{MxO}_3$ (M=Ti, Fe, Mg) Particles as Oxygen Carriers. Energy and
418 Fuels. 2013. 27(3): 1473-1481
- 419 6. Font O, Cordoba P, Lieva C, Romeo LM, Bolea I, Gueada I, Moreno N, Querol X,
420 Fernandez, Diez LI. Fate and abatement of mercury and other trace elements in a
421 coal fluidised bed oxy combustion pilot plant. Fuel 2012; 95:272-81.
- 422 7. Mendiara T, Gayan P, Abad A, Garcia-Labiano F, de Diego LF, Adanez J.
423 Characterisation for disposal of Fe-based oxygen carriers from a CLC unit burning
424 coal. Fuel Processing Technology 2015;138:750-757.
- 425 8. Sathonsaowaphak A, Chindaprasit P and Pimraka K.. Workability and strength of
426 lignite bottom ash geopolymers mortar. Journal of Hazardous Material 2009. (168):
427 45-50
- 428 9. Li Q, Xu H, Li P, Li F, Shen L and Zhai J. Synthesis of geopolymers composites
429 from blends of CFBC fly ash and bottom ashes. Fuel 2012 (97): 366-372.
- 430 10. Bakharev T. Geopolymeric material prepared using class F fly ash and elevated
431 temperature curing. *Cement and Concrete Research*, 2005. (35): 1224-1232
- 432 11. Davidovits, J. 2002. 30 years of successes and failures in geopolymer
433 applications. Market trends and potential breakthroughs. *Keynote Conference on*
434 *Geopolymer Conference*.

- 435 12. Mathekga HI Oboirien BO, Engelbrecht A, North BC and K Premllal.
436 Performance evaluation of South African coals under Oxy-fuel combustion in a
437 Fluidised Bed Reactor. *Energy and Fuels*, 2016 (30):6756-6763
- 438 13. Swanepol JC and Strydom CA... Utilisation of fly ash in a geopolymeric material.
439 *Applied Geochemistry* 2002. (17). 1143-1148
- 440 14. Christopoulos K, Mousios E, Anastasiadou K and Gidaracos E.
441 solidification/stabilization of fly and bottom ash from medical waste incineration
442 facility. *Journal of Hazardous Materials* 2012. (207-208): 165-170
- 443 15. Xu H, Li Q, Shen L, Wang W and Zhai J. synthesis of thermostable geopolymers
444 from circulating fluidized bed combustion (CFBC) bottom ashes. *Journal of*
445 *Hazardous Materials* 2010 (175):198-204
- 446 16. Van Deventer JSJ, Provis JL, Duxson P and Lukey GC. Reaction mechanisms in
447 the geopolymeric conversion of inorganic waste to useful products. *Journal of*
448 *Hazardous Materials* 2007. (139): 506–513
- 449 17. Rosas-CAsarez CA, Arrendondo-Rea SP, Gómez-Soberón JM, Alamaral-Sanchez
450 JL, Corral-Higuer R, Chinchillas-Chinchillas MJ and etc. Experimental study of
451 XRD, FTIR and TGA techniques in geopolymeric materials. *International Journal*
452 *of Advances in Computer Science and Its Applications*,.2014. 4(4). 221-226
- 453 18. Zhang Z, Provis JL, Reid A and Wang H. Fly ash-based geopolymers. The
454 relationship between composition, pore structure and efflorescence. 23rd
455 Australasian Conference on the Mechanics of Structures and Materials
456 (ACMSM23) Byron Bay, Australia, 9-12 December 2014, S.T. Smith (Ed.)
- 457 19. Santa RAAB, Bernardin AM, Humbetro GR and Kuhen NC. Geopolymer
458 synthesized from bottom ash coal ash and calcined paper sludge. *Journal of*
459 *Cleaner Production* 2013. (57): 302-307
- 460 20. Lancelloti I, Cannio M, Ballino F, Catauro M, Barbieri L and Leonelli C.
461 Geopolymers: An option for the valorization of incinerator bottom ash derived
462 “end waste” *Ceramics International* 2015. (41): 2116-2123
- 463 21. Haqn E, Padmanabhan SK and Licciulli A. Synthesis and characteristics of fly ash
464 and bottom ash based geopolymers–A comparative study. *Ceramics International*
465 2014. (40): 2965–2971
- 466 22. Zhu P, Kai G, Kenan F, Sanjayan JG, Wenhui D and Collins F. Damping capacity
467 of fly ash-based geopolymer. 18th International Conference on Composite
468 Materials 2014

- 469 23. Topçu IB and Toprak MU. Properties of geopolymers from circulating fluidized
470 bed combustion coal bottom ash Materials Science and Engineering: A, 2011.
471 (528). 1472-1477
- 472 24. Gou X, Yu QL and Brouwers HJH. Reaction kinetics, gel character and strength of
473 ambient temperature cured alkali activated slag-fly ash blends. Construction and
474 Building Materials 2015. (80). 105-115
- 475 25. Ariož E, Ariož O and Mete Kockar O. leaching of F-type fly ash based
476 geopolymers. Procedia Engineering 2012 (42). 114-1120
- 477 26. Marjanovic N, Komljenovic M, Bascarevic Z and Nikolic V. improving reactivity
478 of fly ash properties of ensuing geopolymers through mechanical activation.
479 Construction and Building Materials 2014 (57). 152-162